Journal of Zhejiang University-SCIENCE B (Biomedicine & Biotechnology) *2022 23(11):943-956*
www.jzus.zju.edu.cn; www.springer.com/journal/11585
E-mail: jzus_b@zju.edu.cn

Research Article

https://doi.org/10.1631/jzus.B2200232

Combination of Se-methylselenocysteine, D-α-tocopheryl succinate, β-carotene, and L-lysine can prevent cancer metastases using as an adjuvant therapy

Yunlong CHENG[1,2*], Shu LIAN[1,3*], Shuhui LI[2], Yusheng LU[1], Jie WANG[2], Xiaoxiao DENG[2], Shengyi ZHAI[2], Lee JIA[1,2,3✉]

[1]*Fujian-Taiwan-Hongkong-Macao Science and Technology Cooperation Base of Intelligent Pharmaceutics, College of Materials and Chemical Engineering, Minjiang University, Fuzhou 350108, China*
[2]*Cancer Metastasis Alert and Prevention Center, Fujian Provincial Key Laboratory of Cancer Metastasis Chemoprevention, College of Chemistry, Fuzhou University, Fuzhou 350002, China*
[3]*Fuzhou Institute of Oceanography, Minjiang University, Fuzhou 350108, China*

Abstract: Objective: Primary tumor treatment through surgical resection and adjuvant therapy has been extensively studied, but there is a lack of effective strategies and drugs for the treatment of tumor metastases. Here, we describe a functional product based on a combination of compounds, which can be used as an adjuvant therapy and has well-known mechanisms for inhibiting cancer metastases, improving anti-cancer treatment, and enhancing immunity and antioxidant capacity. Our designed combination, named MVBL, consists of four inexpensive compounds: L-selenium-methylselenocysteine (MSC), D-α-tocopheryl succinic acid (VES), β-carotene (β-Ca), and L-lysine (Lys). Methods: The effects of MVBL on cell viability, cell cycle, cell apoptosis, cell migration, cell invasion, reactive oxygen species (ROS), and paclitaxel (PTX)-combined treatment were studied in vitro. The inhibition of tumor metastasis, antioxidation, and immune enhancement capacity of MVBL were determined in vivo. Results: MVBL exhibited higher toxicity to tumor cells than to normal cells. It did not significantly affect the cell cycle of cancer cells, but increased their apoptosis. Wound healing, adhesion, and transwell assays showed that MVBL significantly inhibited tumor cell migration, adhesion, and invasion. MVBL sensitized MDA-MB-231 breast cancer cells to PTX, indicating that it can be used as an adjuvant to enhance the therapeutic effect of chemotherapy drugs. In mice, experimental data showed that MVBL inhibited tumor metastasis, prolonged their survival time, and enhanced their antioxidant capacity and immune function. Conclusions: This study revealed the roles of MVBL in improving immunity and antioxidation, preventing tumor growth, and inhibiting metastasis in vitro and in vivo. MVBL may be used as an adjuvant drug in cancer therapy for improving the survival and quality of life of cancer patients.

Key words: Cancer prevention; Cancer metastases; Selenium (Se); Combination of drugs; Nutrition

1 Introduction

Cancer remains the second leading cause of death worldwide (Zhou et al., 2019; Siegel et al., 2022). Although surgical resection can be used for the treatment of primary tumors, cancer patients still face a high risk of tumor recurrence after surgery. Postoperative metastasis is the main cause of death among cancer patients. Drug therapy is the routine treatment for tumors, but has a variety of adverse reactions. Reactive oxygen species (ROS) are oxygen-containing active chemicals produced by chemical reactions in living organisms. A variety of studies have proved that ROS are involved in the malignant transformation of cells (Prasad et al., 2017; Wang et al., 2021). Excessive ROS can induce malignant transformation by regulating transcription factors (c-MYC/p53/hypoxia inducible factor-1α (HIF-1α)) (Crowder et al., 2013), promote tumor cell invasion by targeting kinases and transcription factors, and influence other tumor-associated signaling pathways. Research has shown that tumor

✉ Lee JIA, cmapcjia1234@163.com; jiali@fzu.edu.cn
* The two authors contributed equally to this work
Lee JIA, https://orcid.org/0000-0001-6839-5545

Received Apr. 21, 2022; Revision accepted July 22, 2022; Crosschecked Oct. 16, 2022

cells with high ROS levels have high migration and invasion capacities (Cheung et al., 2020). Antioxidants have been shown to reduce ROS levels in xenograft nude mouse models, and to inhibit hypoxia-induced metastasis in human pancreatic cancer cells (Shimojo et al., 2013; Liu et al., 2015; Guo et al., 2021). ROS can also promote tumor metastasis by modulating lipopolysaccharide-mediated Toll-like receptor 4 (TLR4) signaling in non-small-cell lung cancer (NSCLC). The high levels of ROS in the mitochondria of NSCLC promote cell proliferation, survival, migration, and epithelial-mesenchymal transition by activating extracellular signals to regulate mitogen-activated protein kinase (MAPK) and rat sarcoma virus (Ras)-extracellular signal-regulated kinase (ERK) (Su et al., 2019).

Prevention of tumor metastasis is critical for tumor treatment. After surgery, chemotherapy, and radiotherapy, patients with low immune function and metabolic disorders need exogenous nutrient supplementation to improve their metabolic states and anti-tumor treatment tolerance, and to reduce complications and adverse reactions. Based on this information, we comprehensively analyzed the mechanisms of tumor production, development, and metastasis, and the characteristics of circulating tumor cells (CTCs) in the blood. We then formulated a corresponding preventive and adjuvant treatment, namely MVBL, which contains four components: L-selenium-methylselenocysteine (MSC), D-α-tocopheryl succinic acid (VES), β-carotene (β-Ca), and L-lysine (Lys) (Fig. S1). As early as 2003, the United States Food and Drug Administration (FDA) confirmed that selenium (Se) is a cancer suppressant. Se has an antioxidant effect that inhibits the production of free radicals and reduces the risk of cancer caused by peroxidation (Ørskov and Flyvbjerg, 2000; Fang et al., 2002; Zhou et al., 2007). It also enhances human immune function by promoting lymphocyte proliferation (Avery and Hoffmann, 2018; Jiang et al., 2021) and tumor cell apoptosis (Li et al., 2020; Ganash, 2021). VES, a derivative of vitamin E esterification, is one of the most potent anti-tumor compounds in the vitamin E family. It inhibits multiple cancer-promoting pathways such as nuclear factor-κB (NF-κB) and signal transducer and activator of transcription factor 3 (STAT3) (Jiang, 2017; Huang et al., 2021). β-Ca prevents tumor formation by regulating the levels of cytochrome P450 and glutathione transferase (GST) in vivo (Satomi and Nishino, 2013). It also inhibits the metastasis and invasion of neuroblastoma by decreasing the level of HIF-1α (Kim et al., 2014). Lys is an essential amino acid in the human body. It not only participates in the synthesis of proteins (Ibrahim-Hashim et al., 2011), but also binds to the active site of fibrinogen to reduce fibrinogen production. This protects the tissue matrix by promoting the production of collagen, strengthening the structure of the matrix, reducing the envelopment of connective tissue around tumor cells, and effectively inhibiting the secretion of matrix metalloproteinases (MMPs) (Roomi et al., 2005; Kirchhain et al., 2021). Previous research has focused only on the anti-tumor function of the four compounds individually (Satomi and Nishino, 2013; Jiang, 2017; Ganash, 2021; Kirchhain et al., 2021), and no studies have explored their efficacy in combination for inhibiting tumor metastasis. Thus, a combination of these four substances may not only serve as a nutrient supplement, but also effectively prevent the metastasis of postoperative tumors.

Here, we described a custom-designed combination drug (MVBL), the results of its anti-metastatic and cytotoxic properties, and its effects on tumor cell migration, invasion, and adhesion in vitro. We revealed the enhancement by MVBL of the cancer-inhibiting effect of paclitaxel (PTX). We also analyzed the effects of MVBL on oxidation, immune function, metastasis, and life expectancy in vitro and in vivo.

2 Methods

2.1 MVBL composition and HPLC analysis

MVBL consists of the following substances: MSC (Jiangxi Chuanqi Pharmaceutical Co., Ltd., Nanchang, China), VES (Sigma, St. Louis, USA), β-Ca (Sigma), and Lys (Aladin, Shanghai, China). Drug doses were chosen based on the human doses of each of the four drugs, and converted to mouse doses according to the body surface area index. The structural changes after 24 h mixing of the four components were determined by high-performance liquid chromatography (HPLC; Waters, Milford, USA). HPLC analyses of MSC were carried out using a Waters Atlantis T3 column (4.6 mm×250.0 mm, 5 μm), with pure water as the mobile phase. The flow rate was set at

1.0 mL/min. The injection volume was 20 μL and the column temperature was 35 ℃. HPLC analyses of VES were carried out using a Waters EclipseXDB-C18 column (4.6 mm×250.0 mm, 5 μm), and the mobile phase consisted of methanol (Merco, USA) and acetic acid solution (Sinopharm Chemical Reagent Co., Ltd., Shanghai, China) (volume ratio at 500:3.2). The flow rate was set at 0.8 mL/min. The injection volume was 20 μL and the column temperature was 30 ℃. HPLC analyses of β-Ca were carried out using the same column and mobile phase, with acetonitrile (Merco) and trichloromethane (Sinopharm Chemical Reagent Co., Ltd.) (volume ratio at 85:12.3) solution. The flow rate was set at 1.5 mL/min. The injection volume was 20 μL and the column temperature was 35 ℃.

2.2 Cell culture

Human breast cancer cells MDA-MB-231 and MCF-7, human lung cancer cells A549, mouse breast cancer cells 4T1, human colon cancer cells HT29, human normal liver cells LO2, and human lung fiber cells HELF were purchased from the Type Culture Collection of the Chinese Academy of Sciences (Shanghai, China). The MCF-7, A549, 4T1, and LO2 cells were cultured in Roswell Park Memorial Institute (RPMI) 1640 medium (Gibco, Carlsbad, USA). MDA-MB-231 and HELF cells were grown in Dulbecco's modified Eagle's medium (DMEM; Hyclone, Logan, USA). All cells were cultured in medium containing 10% (volume fraction) fetal bovine serum (FBS; Gibco) and 1% (volume fraction) penicillin/streptomycin (Gibco) in a humidified atmosphere with 5% CO_2 at 37 ℃.

2.3 Cell viability assay

Cytostatic effects were determined using the 3-(4,5-dimethylthiazol-2-yl)-2,5-diphenyltetrazolium bromide (MTT) assay. Cells were seeded into 96-well plates at 1×10^4 cells/well. After incubating at 37 ℃ for 24 h, the supernatant was replaced with medium containing different concentrations of single drugs or MVBL, and five-replicate wells were set for each sample. After 24 h, the medium was aspirated, MTT solution was added for 4 h, and finally formazan was dissolved in dimethyl sulfoxide (DMSO). Cell viability was calculated from the absorbance, which was measured using a microplate reader (490 nm/570 nm).

2.4 Cell cycle and apoptosis assays

The cell cycle was detected by staining nuclei with propidium iodide (PI). A549, MCF-7, and MDA-MB-231 cells were seeded in six-well plates and incubated with single drugs and different concentrations of MVBL (Table 1). After 24 h, the cells were harvested and centrifuged, washed twice with pre-cooled phosphate-buffered saline (PBS), and fixed in 70% (volume fraction) ice-cold ethanol overnight. After centrifuging the ethanol, 500 μL of prepared PI was added to each tube, which was then left in the dark at 37 ℃ for 40 min. The cell cycle distribution was determined by flow cytometry (BD Biosciences, NJ, USA) with laser excitation set at 488 nm.

Table 1 Drug concentrations in cell cycle, apoptosis, and ROS experiments

Group	MSC (μmol/L)	VES (μmol/L)	β-Ca (μmol/L)	Lys (μmol/L)
Control	0	0	0	0
MSC	10			
VES		20		
β-Ca			20	
Lys				200
Low MVBL	2	4	4	40
Medium MVBL	5	10	10	100
High MVBL	10	20	20	200

ROS: reactive oxygen species; MSC: L-selenium-methylselenocysteine; VES: D-α-tocopheryl succinic acid; β-Ca: β-carotene; Lys: L-lysine.

Consistent with the cell cycle dosing method described above, the supernatant medium was collected after incubation with the drugs for 24 h, and centrifuged with the harvested cells. After washing twice with pre-cooled PBS, 500 μL of binding buffer, 5 μL of Annexin-V fluorescein isothiocyanate (FITC), and 10 μL of PI were added to each tube. The cells were incubated for 15 min at room temperature in the dark, and detected by flow cytometry (BD Biosciences).

2.5 Cell migration and cell invasion assays

The cells were seeded in 12-well plates. After a monolayer of cells completely covered the bottom of each well, three cell lines were drawn vertically in each well and washed with 2% (volume fraction) PBS, and then different concentrations of MVBL (Table 2, low/high) were added. The scratch width of each well was observed under a fluorescence microscope at 0 h and 24 h, and the migration distances in MVBL and the control group were calculated and compared.

Table 2 Drug concentrations for cell migration and invasion assays

Group	MSC (μmol/L)	VES (μmol/L)	β-Ca (μmol/L)	Lys (μmol/L)
Control	0	0	0	0
Low MVBL	2	4	4	40
High MVBL	5	10	10	100

MSC: L-selenium-methylselenocysteine; VES: D-α-tocopheryl succinic acid; β-Ca: β-carotene; Lys: L-lysine.

The invasive ability of the cells was examined by transwell experiments. Matrigel was first placed at the bottom of the chamber, and then the MVBL-containing medium was prepared using incomplete medium containing 0.1% (1 g/L) bovine serum albumin (BSA) and suspended cells. Each chamber was added with 250 μL of the cell suspension containing MVBL. Outside of the chamber, 750 μL of 20% (volume fraction) FBS-containing medium was added, and the culture was continued for 24 h. Five fields were randomly selected under the microscope and photographed, and the number of cells penetrating the chamber was counted for each treatment.

2.6 Analyses of the effects of combined MVBL and PTX treatment on cell cytotoxicity, cell cycle, and apoptosis

Cell cytotoxicity, cell cycle, and apoptosis experiments were used to detect the effects of MVBL combined with PTX. We determined the inhibition of PTX (0.2, 0.4, 0.8, 1.6, 3.2, 6.4, 12.5, 25.0, and 50.0 μmol/L) for 24 h on breast cancer cells (MDA-MB-231) by MTT assay. Based on MTT results, the best PTX concentration was combined with different MVBL concentrations. The effects of PTX plus different MVBL concentrations on the cell cycle and apoptosis were tested by flow cytometry (BD FACSAria™ III). Cell cycle and apoptosis experimental methods are described in Section 2.4.

2.7 Analyses of the effects of MVBL on ROS in tumor cells

Different concentrations of MVBL were incubated with 1×10^5 MCF-7 cells in a six-well plate for 24 h. After incubation, cells from each well were collected in a centrifuge tube and washed three times with PBS. The prepared 2',7'-dichlorodihydrofluorescein-diacetate (DCFH-DA) was added and incubated at 37 ℃ for 20 min. After staining was completed, cells were washed three times with PBS, and tested using a flow cytometer (BD FACSAria™ III) with laser detection at a wavelength of 488 nm.

2.8 In vivo analyses of antioxidant capacity and immunity

Kunming mice (females, aged 6–8 weeks) were purchased from the Shanghai Laboratory Animal Co., Ltd. (SLAC, Shanghai, China). They were randomly divided into four groups (n=10), including a control group and three MVBL groups (low, medium, and high) (drug dosing shown in Table 3). VES and β-Ca were dissolved in oil, MSC and Lys were dissolved in water, and then the two solutions were mixed to form an oil-water mixture. The mice were orally inoculated with 200 μL of the mixture for 30 consecutive days. The mice were weighed the day before gavage, and weighed once every 3 d until the 30th day of gavage.

Table 3 Drug dosage of each mice group

Group	MSC (mg/kg)	VES (mg/kg)	β-Ca (mg/kg)	Lys (mg/kg)
Control	0	0	0	0
Low MVBL	0.008	18	0.24	8
Medium MVBL	0.040	90	1.20	40
High MVBL	0.200	450	6.00	200

MSC: L-selenium-methylselenocysteine; VES: D-α-tocopheryl succinic acid; β-Ca: β-carotene; Lys: L-lysine.

2.9 Immunity assay

Flow cytometry was used to detect the changes in T cells in the mice. Blood was taken from the eyelids on Days 0 and 15 after intragastric administration, and the anticoagulant ethylene diamine tetraacetie acid (EDTA) was added. And then, 1.25 μL of CD8a-perCP antibody and 2.5 μL of CD3e-PE antibody were added, and the samples were incubated for 20 min. Ammonium-chloride-potassium (ACK) lysis buffer was then added to remove the red blood cells, and the samples were incubated for 3 min before being centrifuged at 400g for 5 min, and this step was carried out three times. Then, 400 μL of PBS containing 1% (volume fraction) FBS was added, and the samples were analyzed by flow cytometry (488 nm). The proportions of T cells were recorded.

Two hours after the last gavage, the mice were injected with India ink (0.01 mL/g) in the tail vein. At the 2nd and 8th minutes, 10 μL of blood was taken from the orbit, and 1 mL of 0.1% (1 g/L) Na_2CO_3 was

added. The absorbance was then measured using a microplate reader at 580 nm. The carbon clearance (K) was calculated as $K=(\lg A_1-\lg A_2)/(t_2-t_1)$, where t_1 is the 2nd minute, t_2 is the 8th minute, A_1 is the absorbance of the blood sample taken at the 2nd minute, and A_2 is the absorbance of the blood sample taken at the 8th minute. After blood was collected, the mice were weighed and sacrificed. The spleen was dissected from each mouse and weighed to calculate the spleen index (spleen index=(spleen weight/mouse weight)×10).

2.10 Antioxidant capacity assay

Blood was taken from the eyelids on the 15th and 30th days after intragastric administration, and 4% (volume fraction) sodium citrate was added for anticoagulation. The samples were then centrifuged at 600*g* for 10 min at 4 ℃. The serum supernatant was collected and stored at −80 ℃.

First, the total antioxidant capacity (T-AOC) of each sample was measured. $FeSO_4\cdot 7H_2O$ standard solutions (1.5, 1.2, 0.9, 0.6, and 0.3 mmol/L) and 2,4,6-tripyridyl-*S*-triazine (TPTZ)-containing ferric reducing antioxidant power (FRAP) working solutions were prepared. A total of 5 μL of $FeSO_4$ was added to 180 μL of each FRAP working solution to make a standard solution. For each sample, 5 μL of serum was added to 180 μL of FRAP working solution, and 5 μL of ultrapure water was added for the control group. The solutions were placed in 96-well plates and tested at 593 nm. The T-AOC in the blood was determined by calculating the TPTZ content.

Second, the malondialdehyde (MDA) content in the blood was measured. Briefly, 200 μL of MDA detection working solution, 50 μL of serum (control, low, medium, and high), and 50 μL of PBS for the blank control or 50 μL of standard solution (1, 2, 5, 10, 20, and 50 μmol/L) were added to centrifuge tube. The samples were incubated at 100 ℃ for 15 min and then centrifuged at 100*g* for 5 min. The supernatant was removed and added to a 96-well plate for detection with a microplate reader (450 nm). The MDA content was calculated according to the standard curve.

Finally, superoxide dismutase (SOD) activity in the blood was measured. A total of 151 μL of SOD detection buffer, 8 μL of water soluble tetrazolium-8 (WST-8, a kind of total SOD activity detection reagent), and 1 μL of enzyme solution were mixed to make a WST-8 working solution. There were six samples: (1) control 1 (SOD detection buffer 20 μL+WST-8 working solution 160 μL+initiation solution 40 μL), (2) control 2 (WST-8 working solution 160 μL+initiation solution 40 μL), (3) control 3 (control serum 20 μL+WST-8 working solution 160 μL+initiation solution 20 μL), (4) low (low serum 20 μL+WST-8 working solution 160 μL+initiation solution 20 μL), (5) medium (medium serum 20 μL+WST-8 working solution 160 μL+initiation solution 20 μL), and (6) high (high serum 20 μL+WST-8 working solution 160 μL+initiation solution 20 μL). The absorbance was measured at 450 nm with a microplate reader.

The SOD inhibition rate (IR) and the SOD enzyme activity were calculated using the following formulas:

$$\mathrm{IR}=[(A_{\text{control 1}}-A_{\text{control 2}})-(A_{\text{sample}}-A_{\text{control 3}})]/(A_{\text{control 1}}-A_{\text{control 2}})\times 100\%,$$

$$\text{SOD enzyme activity}=\mathrm{IR}/(1-\mathrm{IR}).$$

2.11 In vivo metastasis analysis

All animal experiments were performed in accordance with animal protocol procedures approved by the Institutional Animal Care and Use Committee (IACUC) of Minjiang University (Fuzhou, China). BALB/c mice (females, aged 6–8 weeks) were purchased from Shanghai Laboratory Animal Co., Ltd. They were randomly divided into four groups (n=6), which received an intravenous injection of PBS (200 μL, pH=7.4) containing 4T1 cells (5.0×10^4) into the tail vein. The mice were sacrificed 15 d after gavage of the same dose as above, and their lungs were dissected and placed in Bouin's solution for 24 h for pulmonary nodule counting.

2.12 Statistical analysis

Statistical differences were analyzed using Statistical Package for the Social Sciences (IBM SPSS, Statistics 25, Chicago, IL, USA) based on one-way analysis of variance (ANOVA), for comparison among three groups and more than three samples per group or unpaired Student's t-test for comparison between two groups and more than three samples per group.

3 Results

3.1 Inhibition of tumor cell activity by MVBL

MVBL is composed of four compounds including MSC, VES, β-Ca, and Lys. HPLC results (Fig. S2)

showed that there was no mutual reaction among them after mixing for 24 h, and their properties were stable. We firstly examined the inhibitory effects of MSC, VES, β-Ca, Lys, and MVBL on several tumor cell lines, including A549, MDA-MB-231, HT-29, MCF-7, and 4T1 to determine the best concentration for MVBL. The MTT assay results showed the sensitivity of the different cells to β-Ca, Lys, VES, and MSC (Figs. 1a–1d). A high concentration of β-Ca was the most toxic to 4T1, HT29, A549, and MDA-MB-231 cells, but there was no obvious toxicity to any tumor cells at lower concentrations (Fig. 1a). Lys had low toxicity to all cells (Fig. 1b), with all showing cell viability higher than 80%. VES had the most obvious toxicity to LO2, 4T1, HT-29, and MDA-MB-231 cells (Fig. 1c). Only A549 and 4T1 cells were sensitive to MSC (Fig. 1d). We tested the effects of β-Ca, Lys, VES, and MSC on normal cells, such as LO2 and HELF cells. The drugs showed lower toxicity to normal cells than to tumor cells (Figs. 1a–1d). The combination of the four compounds, MVBL, had obvious inhibitory effects on various tumor cell types at different concentrations (Fig. 1e and Table 4). Significantly, the cell viability of A549 cells after treatment with the 5th concentration of MVBL (with concentrations of MSC, VES, β-Ca, and Lys of 30, 60, 60, and 600 μmol/L, respectively) was about 50%–60%, while each single compound showed no cytotoxicity to A549 cells at that concentration. The cell viability experiments

Table 4 Single drug and MVBL concentrations for cell viability

Group	No.	MSC (μmol/L)	VES (μmol/L)	β-Ca (μmol/L)	Lys (μmol/L)
Control	0	0	0	0	0
MVBL	1	2	4	4	40
	2	5	10	10	100
	3	10	20	20	200
	4	20	40	40	400
	5	30	60	60	600
	6	35	70	70	700
	7	40	80	80	800
	8	45	90	90	900
	9	50	100	100	1000

MSC: L-selenium-methylselenocysteine; VES: D-α-tocopheryl succinic acid; β-Ca: β-carotene; Lys: L-lysine; MVBL: combination of drugs (MSC, VES, β-Ca, and Lys).

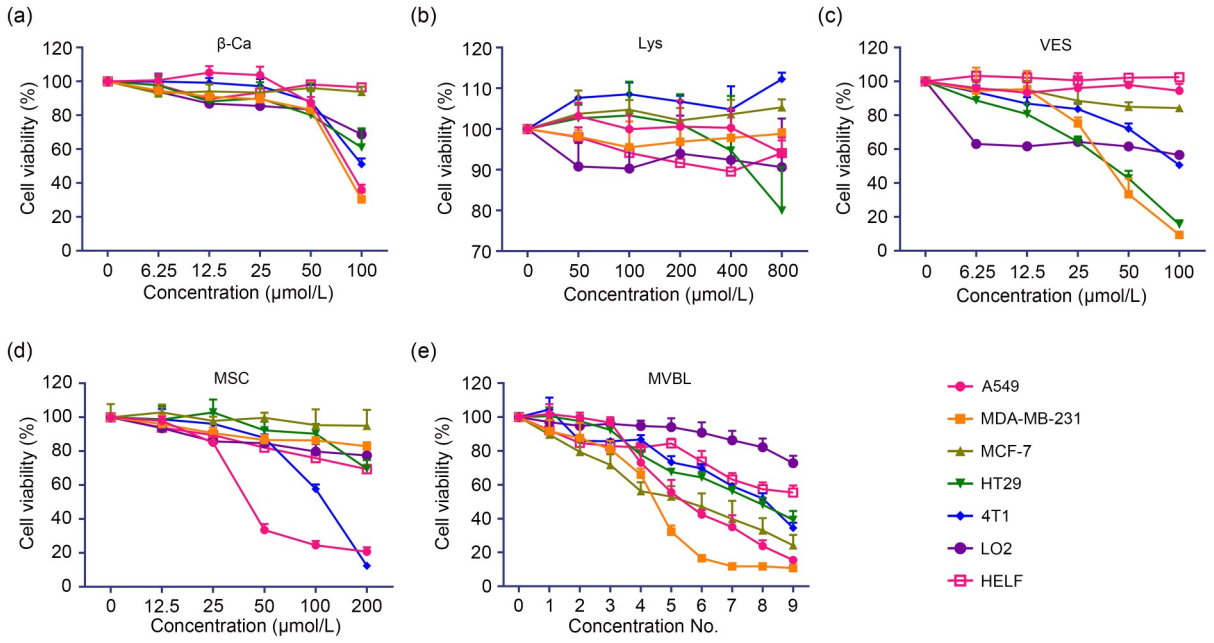

Fig. 1 Cytotoxicities of β-Ca, Lys, VES, MSC, and MVBL toward various cell types. All cells were treated for 24 h. (a) Effects of β-Ca on the viability of seven types (A549/HT29/MDA-MB-231/MCF-7/4T1/LO2/HELF) of cells. (b) Effects of Lys on the viability of seven types of cells. (c) Effects of VES on the viability of seven types of cells. (d) Effects of MSC on the viability of seven types of cells. (e) Effects of MVBL on the viability of seven types of cells. The data are represented as mean±standard deviation (n=5). The details of MVBL concentration Nos. are shown in Table 4. β-Ca: β-carotene; Lys: L-lysine; VES: D-α-tocopheryl succinic acid; MSC: L-selenium-methylselenocysteine; MVBL: combination of drugs (MSC, VES, β-Ca, and Lys).

demonstrated that the 5th concentration of MVBL was more lethal to tumor cells than the single drugs.

3.2 Effects of MVBL on the cell cycle and apoptosis

The cell cycle and apoptosis are important for tumor cell growth and proliferation, so we examined the effects of different concentrations of MVBL on the cell cycle and apoptosis in A549, MCF-7, MDA-MB-231, and 4T1 tumor cells (Table 1). The results showed that MVBL induced no obvious cell cycle arrest of A549 (Figs. 2a and 2b), MCF-7 (Figs. S3a and S6), MDA-MB-231 (Figs. S4a and S6), or 4T1 (Figs. S5a and S6) cells. High concentrations of MVBL led to substantial apoptosis in A549 (Figs. 2c and 2d) and MDA-MB-231 cells (Figs. S4b and S7), but there was no apoptosis of MCF-7 (Figs. S3b and S7) or 4T1 (Figs. S5b and S7) cells.

The high concentrations of MVBL were used to alter the behavior of CTCs by inhibiting cell proliferation, such as by inhibiting tumor metastasis without killing tumor cells, and to minimize side effects.

3.3 Inhibition of migration and invasion by MVBL

Migration and invasion are important processes in tumor metastasis. Cancer metastasis may therefore be inhibited through the suppression of tumor cell migration and invasion. To measure the ability of MVBL to inhibit migration, scratch assays were conducted.

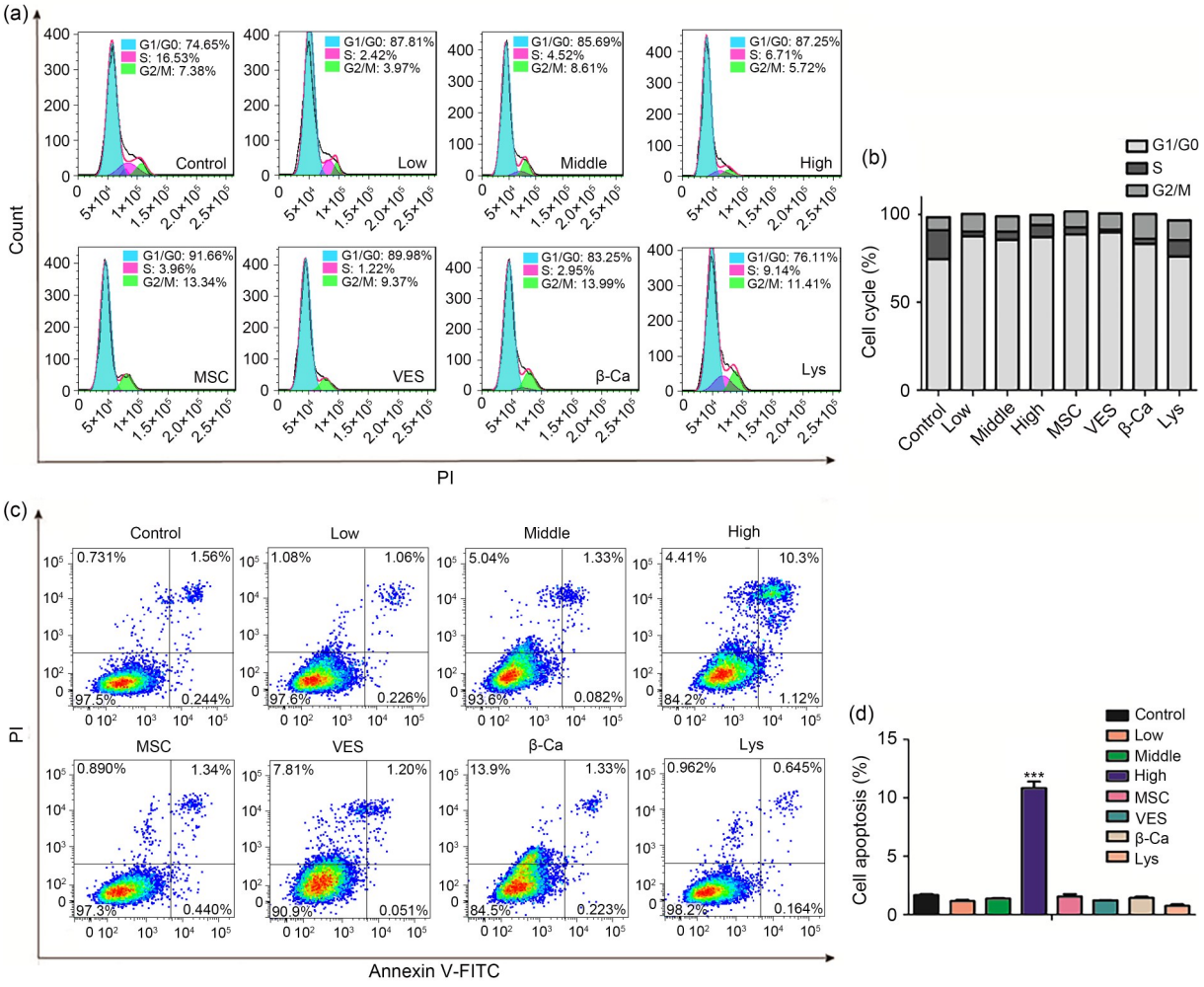

Fig. 2 Cell cycle and apoptosis of MVBL and single drugs in A549 cells. (a) Effects of MVBL and single drugs on the cell cycle in A549 cells. (b) Column chart of cell cycle. (c) Effects of MVBL and single drugs on the cell apoptosis in A549 cells. (d) Column chart of cell apoptosis, in which the data are represented as mean±standard deviation (n=3). *** P<0.001, vs. control. MVBL: combination of drugs (MSC, VES, β-Ca, and Lys); β-Ca: β-carotene; Lys: L-lysine; VES: D-α-tocopheryl succinic acid; MSC: L-selenium-methylselenocysteine; PI: propidium iodide; FITC: fluorescein isothiocyanate.

Compared with the control, MVBL significantly inhibited the migration of A549, MCF-7, and MDA-MB-231 cells (Fig. 3a), decreasing mobility by 18%, 12%, and 15% at low concentrations, and 38%, 24%, and 29% at high concentrations, respectively. Transwell assays were used to verify the inhibition of tumor cell invasion by MVBL. The numbers of cells penetrating the chambers decreased significantly upon treatment with different MVBL concentrations (Fig. 3b). Combined with the results of the cytotoxicity assays, these results indicated that MVBL inhibited tumor cell migration, adhesion, and invasion at the selected concentration, but did not kill the cells.

3.4 Sensitivity of tumor cells to PTX by MVBL

PTX, a first-line treatment drug for breast cancer, has greater side effects and induces greater drug resistance when used at high doses. The MTT assay results showed that low concentrations of PTX did not have strong lethal effects on MDA-MB-231 cells (Fig. 4a). The cell survival rates were 55% (6.25 μmol/L PTX) and 51% (12.5 μmol/L PTX). We chose a low concentration (6.25 μmol/L) PTX to study the synergistic effect of PTX and MVBL. This dose had a certain inhibitory effect on tumor cells, but fewer side effects than the higher doses (Fig. 4b). The results indicated that when PTX was used in combination with

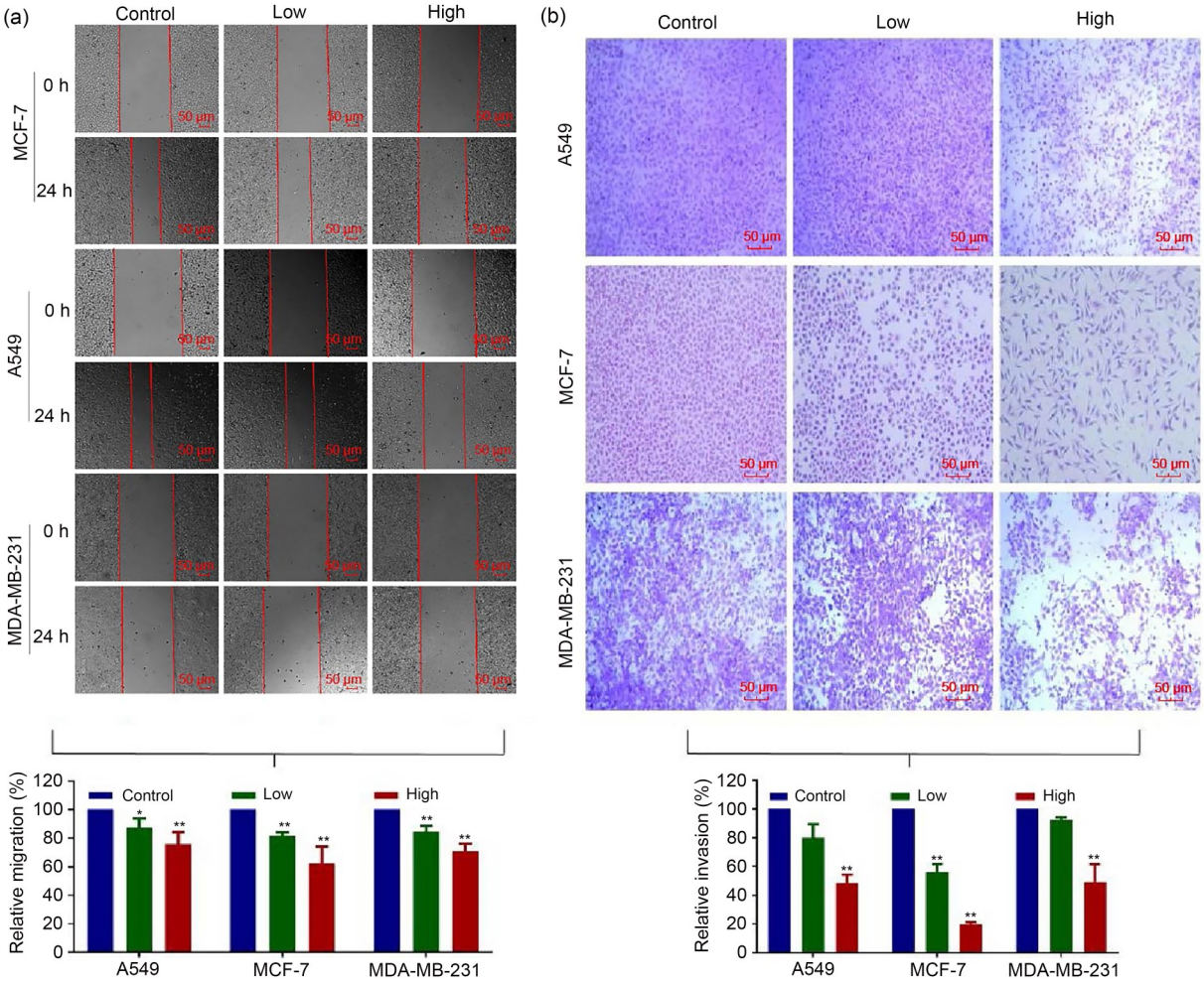

Fig. 3 Inhibition of A549, MCF-7, MDA-MB-231 cell migration and invasion by MVBL. After 24 h of treatment at selected low and high concentrations, the effect was found to increase with concentration. (a) The cell migration distance of the treated cells was shorter than that of the control cells. (b) The numbers of cells passed through the membrane after treatment with different drug concentrations. The data are represented as mean±standard deviation (n=3). * P<0.05, ** P<0.01, vs. control. MVBL: combination of drugs (MSC, VES, β-Ca, and Lys); MSC: L-selenium-methylselenocysteine; VES: D-α-tocopheryl succinic acid; β-Ca: β-carotene; Lys: L-lysine.

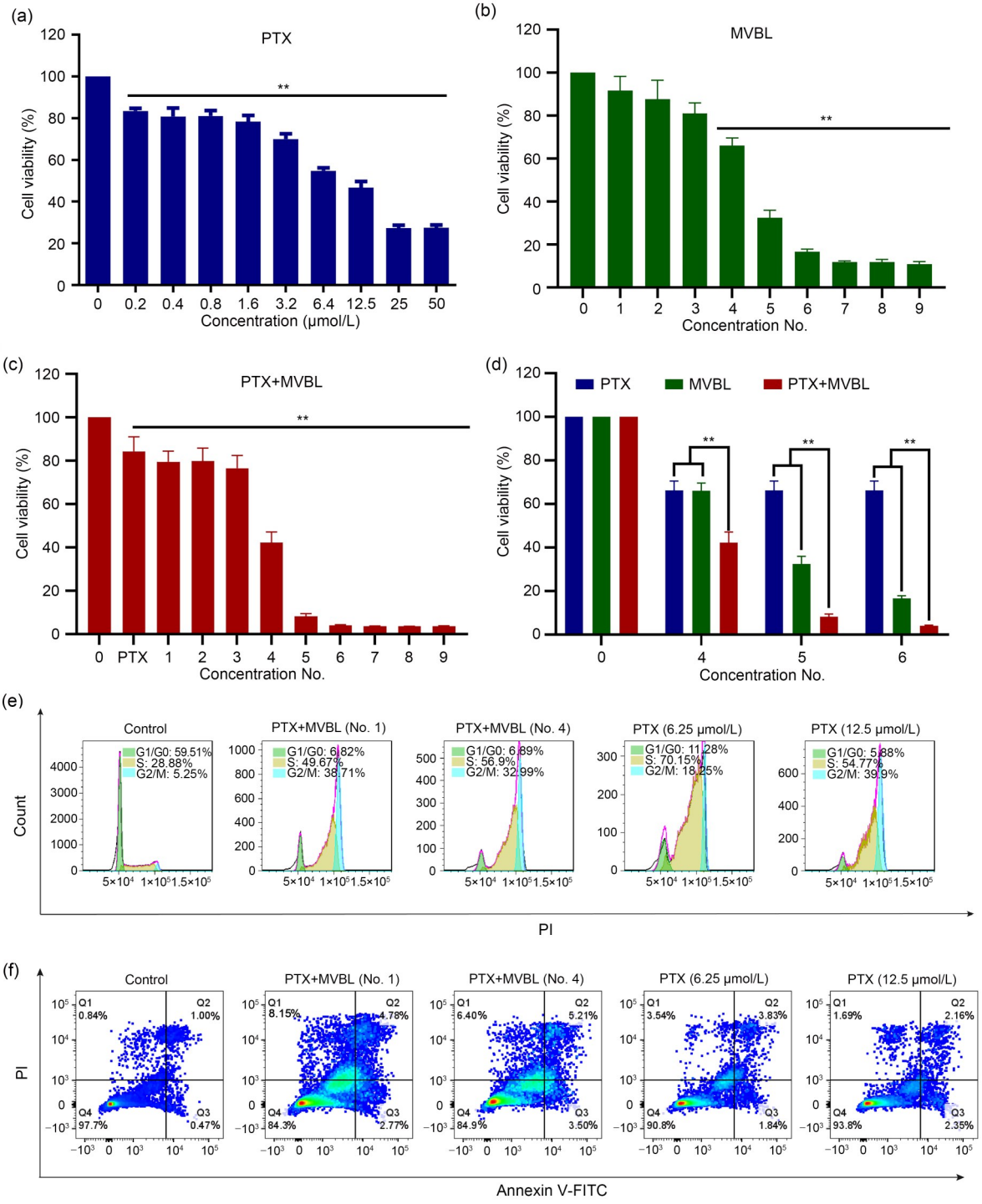

Fig. 4 Effects of MVBL combined with PTX on MDA-MB-231 cells. The cells were incubated with the drugs for 24 h. (a) The cells were treated with PTX. (b) The cells were treated with MVBL. (c) The cells were treated with PTX (6.25 μmol/L) combined with different concentrations of MVBL (Nos. 1–9). (d) The cells were treated with PTX (6.25 μmol/L) combined with MVBL (Nos. 4–6). (e) Cell cycle distributions (control, PTX (6.25 μmol/L)+MVBL (No. 1), PTX (6.25 μmol/L)+MVBL (No. 4), PTX (6.25 μmol/L), and PTX (12.5 μmol/L)). (f) Apoptosis (control, PTX (6.25 μmol/L)+MVBL (No. 1), PTX (6.25 μmol/L)+MVBL (No. 4), PTX (6.25 μmol/L), and PTX (12.5 μmol/L)). The details of MVBL concentration Nos. are shown in Table 5. The data are represented as mean±standard deviation (n=5). $^{**}P$<0.01, vs. control. MVBL: combination of drugs (MSC, VES, β-Ca, and Lys); PTX: paclitaxel; β-Ca: β-carotene; Lys: L-lysine; VES: D-α-tocopheryl succinic acid; MSC: L-selenium-methylselenocysteine; PI: propidium iodide; FITC: fluorescein isothiocyanate.

MVBL, it was the most toxic to MDA-MB-231 cells (Figs. 4c and 4d). We then examined the effects of different MVBL groups (Table 5) on cell proliferation by flow cytometry. The results revealed that MVBL combined with PTX (6.25 μmol/L) exerted the same effect as 12.5 μmol/L PTX alone, and more cells were retained in the S phase and the G2/M phase after combined treatment than after single-drug treatment (Fig. 4e). In addition, more apoptosis occurred in the group treated with MVBL combined with 6.25 μmol/L PTX than in the group treated with 12.5 μmol/L PTX alone (Fig. 4f). These results indicated that MVBL could enhance the killing effect of PTX on tumor cells, specifically by reducing cell survival, promoting apoptosis, and inhibiting cell proliferation.

Table 5 Drug concentration for cell viability, cell cycle, and apoptosis

Group No.	MSC (μmol/L)	VES (μmol/L)	β-Ca (μmol/L)	Lys (μmol/L)	PTX (μmol/L)
0	0	0	0	0	0
1	2	4	4	40	6.25
2	5	10	10	100	6.25
3	10	20	20	200	6.25
4	20	40	40	400	6.25
5	30	60	60	600	6.25
6	35	70	70	700	6.25
7	40	80	80	800	6.25
8	45	90	90	900	6.25
9	50	100	100	1000	6.25

MSC: L-selenium-methylselenocysteine; VES: D-α-tocopheryl succinic acid; β-Ca: β-carotene; Lys: L-lysine; PTX: paclitaxel.

3.5 Effect of MVBL on ROS levels

In addition to Lys, the remaining three ingredients in MVBL have strong antioxidant capacities. DCFH-DA is a non-labelled oxidation-sensitive probe that can be hydrolyzed by intracellular esterase to form DCFH. It can be oxidized by intracellular ROS to form 2',7'-dichlorofluorescein (DCF), which is fluorescent. Therefore, the intensity of DCF fluorescence measured by flow cytometry can be used to determine the intracellular ROS content. ROS levels in MCF-7 cells decreased with increasing MVBL concentration (Fig. 5a). Excessive ROS levels increased the malignant metastasis of tumors. MVBL could reduce the levels of free oxygen species in cells and thereby reduce the probability of tumor metastasis.

3.6 Effect of MVBL on antioxidant capacity in vivo

Due to metabolic abnormalities, the levels of ROS are higher in tumor tissues than those in normal tissues, and this plays an important role in the occurrence and development of tumors. Here, we collected blood from the eyelids of mice on Days 15 and 30 after gavage to detect the relationships between treatment duration/dose and T-AOC, SOD, and MDA levels. As shown in Fig. 5b, after 15 d of gavage, the T-AOC levels of the low-, medium-, and high-dose groups were respectively 1.44, 1.66, and 1.98 times of the control group, and after 30 d were 1.47, 3.04, and 3.83 times of the control group, respectively. Therefore, the T-AOC in mouse plasma was enhanced with increasing dose and prolonged administration time. SOD levels in mouse plasma also increased with time and dose. Analyses of these two indicators showed that the antioxidant capacity of mice was getting strong with treatment. MDA is another indicator of oxidative capacity. Specifically, it is an indicator of lipid membrane peroxidation in mice. Contrary to the situations for T-AOC and SOD, a higher MDA content indicated a higher degree of oxidation. Fig. 5b revealed that MDA decreased with time and dose. The above data showed that MVBL had a strong antioxidation capacity.

3.7 Effect of MVBL on immunity in vivo

We tested the immunity of mice after treatment with MVBL in two ways. First, we measured the changes in carbon particle clearance and spleen weight in the control and experimental groups. Second, we determined the changes in the proportion of T cells in the blood. After carbon particles were injected into the tail vein of mice, the blood flowed to the liver and spleen, where the particles were phagocytosed and eliminated by macrophages. The carbon particle clearance index increased with the dose of MVBL (Fig. 5c). Spleen weight was also increased after MVBL treatment, and it was the heaviest in the medium-dose group. The spleen weight of mice in the high-dose group was lower than medium-dose group, probably because of the higher absorption burden (Fig. 5d). The proportion of T lymphocytes in the medium-dose group was also improved compared with that in the untreated group (Fig. 5e). The results of these three experiments suggested that MVBL had the ability to enhance the immune function of mice, enabling them to resist disease with their own immune systems.

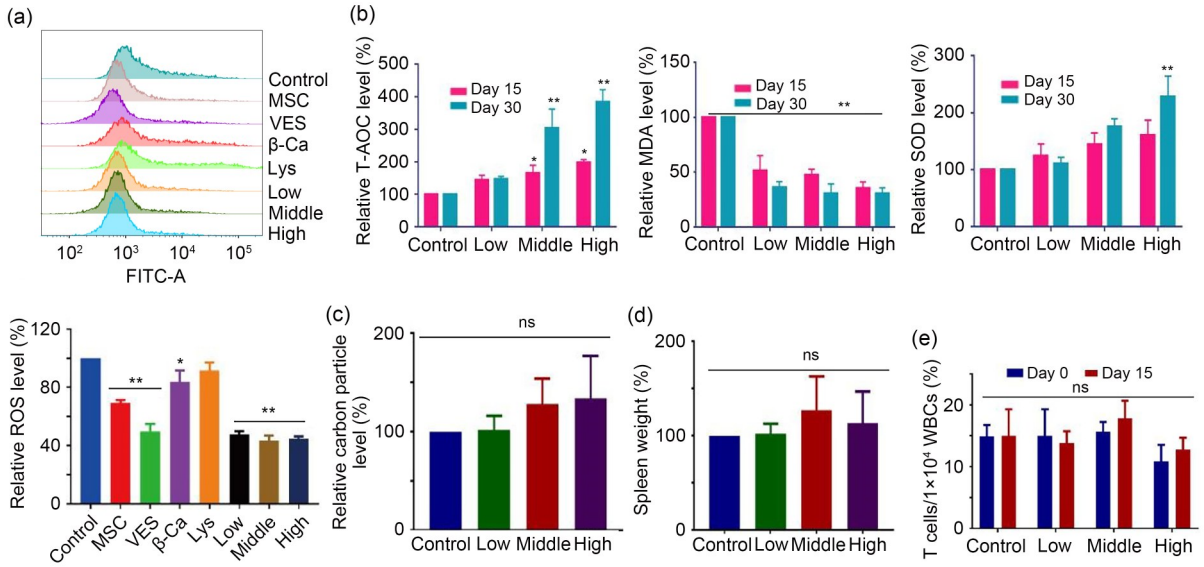

Fig. 5 Results of oxidative and immune function studies. (a) Effects of MVBL and single drugs on ROS levels in MCF-7 cells after 24 h. (b) Changes in T-AOC/MDA/SOD levels on Days 15 and 30 after dosing in vivo. (c) Carbon clearance. (d) Spleen weight. (e) Number of T cells per 1×10^4 WBCs as detected by flow cytometry on Days 0 and 15. The data are represented as mean±standard deviation (n=10). * P<0.05, ** P<0.01, ^{ns} P>0.05, vs. control. MVBL: combination of drugs (MSC, VES, β-Ca, and Lys); ROS: reactive oxygen species; T-AOC: total antioxidant capacity; MDA: malondialdehyde; SOD: superoxide dismutase; WBCs: white blood cells; FITC: fluorescein isothiocyanate; β-Ca: β-carotene; Lys: L-lysine; VES: D-α-tocopheryl succinic acid; MSC: L-selenium-methylselenocysteine; ns: not significant.

3.8 Effect of MVBL on cancer metastasis in vivo

To determine the inhibitory effect of MVBL on tumor metastasis in vivo, we formed a lung metastasis model by injecting 4T1 cells into the tail veins of mice, and counted the tumor nodes in the lungs after 15 d. The average number of lung nodules in the control group was 76, while the average number in the low-, medium-, and high-dose groups were 73, 49, and 45, respectively (Fig. 6c). The average number of lung nodules decreased with increasing dose. As shown by the survival curve (Fig. 6a), the middle dose of MVBL significantly prolonged the survival time of mice. Compared with the control group, the three experimental groups exhibited ameliorative effects, and the medium-dose treatment was the most effective. During the experiment, there were no obvious differences in mouse body weight changes (Fig. 6b).

4 Discussion

In tumor patients, the infinite proliferation of tumor cells and metabolic disorder of the body consume a large amount of nutrients and energy (Dikic and Elazar, 2018; Martínez-Reyes and Chandel, 2021), resulting in malnutrition and abnormal energy-nutrient metabolism, directly affecting their cells and tissues. In this article, we propose a new combination of drugs, MVBL, to inhibit cancer metastasis. We proved that MVBL can improve the physical condition and prolong the survival time of patients by increasing their antioxidant capacity and supplementing their nutrition.

MVBL contains four components (Fig. S1): MSC, VES, β-Ca, and Lys, which are rich in antioxidant (Prasad et al., 2017; Cheung et al., 2020), antitumor (Li et al., 2020; Ganash, 2021; Guo et al., 2021), and nutritional supplementation (Marian and August, 2014) functions. It is reported that β-Ca and MSC can inhibit adhesion, invasion, migration, and lung metastasis of hepatoma cells (Ma et al., 2017; Jiang et al., 2021). We demonstrated that MVBL had excellent inhibitory effects on a variety of tumor cell types, including A549, MDA-MB-231, HT29, 4T1, and MCF-7 cells (Figs. 1, 2, and S3–S7). The inhibition of migration, adhesion, and invasion indicated that MVBL could reduce the metastatic capacity of tumor cells (Fig. 3), and which is also expected to inhibit the metastasis of CTCs in vivo. It was reported that tumors are prone to

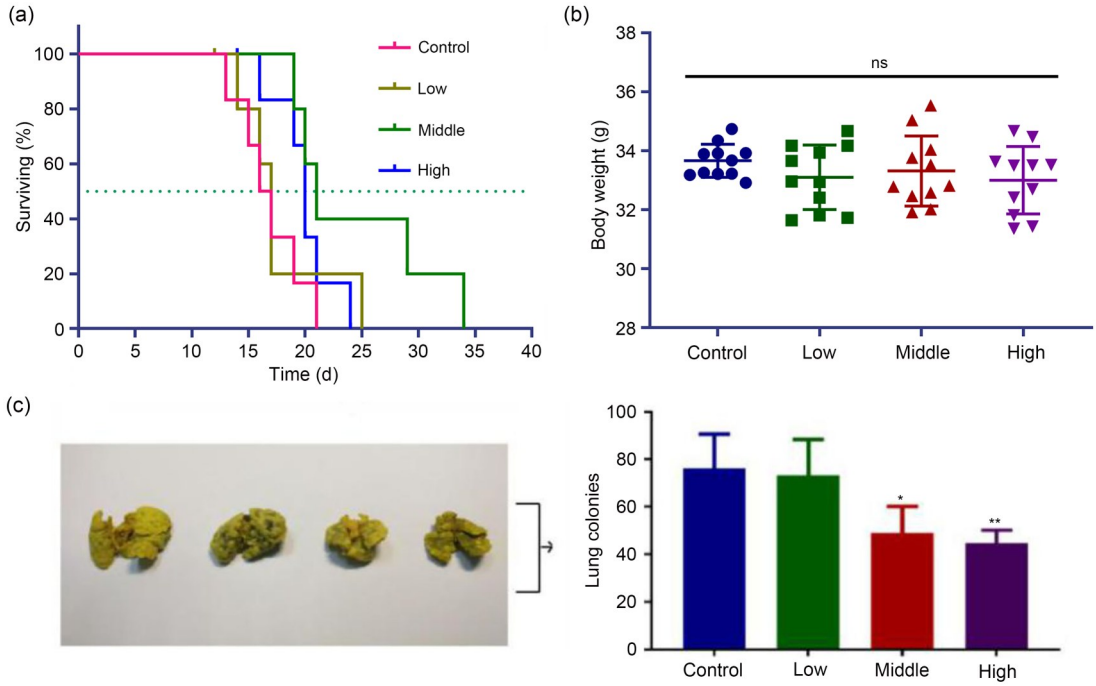

Fig. 6 Inhibition of tumor metastasis by MVBL in vivo. (a) Average survival time of mice in the control group (16.5 d), the low-dose group (17 d), the medium-dose group (21 d), and the high-dose group (20 d). (b) Mouse weight. (c) Number of lung metastases. The data are represented as mean±standard deviation (n=6). $^{*}P$<0.05, $^{**}P$<0.01, ^{ns}P>0.05, vs. control. MVBL: combination of drugs (MSC, VES, β-Ca, and Lys); β-Ca: β-carotene; Lys: L-lysine; VES: D-α-tocopheryl succinic acid; MSC: L-selenium-methylselenocysteine; ns: not significant.

develop resistance to chemotherapy drugs such as PTX (Abu Samaan et al., 2019). In our study, MVBL combined with PTX significantly improved the anti-tumor efficacy of low concentration PTX without obvious side effects (Fig. 4). These results indicated that MVBL may be used as an adjuvant chemotherapy drug in the treatment of tumors. Recent research has demonstrated that higher ROS levels are associated with higher cell migration and invasion capacities (Cheung et al., 2020). Our results proved that MVBL significantly improved antioxidant capacity both in vivo and in vitro (Fig. 5), and the associated reductions in ROS helped to inhibit tumor growth and metastasis (Zhang et al., 2019). At the animal level, MVBL was able to significantly inhibit tumor metastasis in a mouse lung metastasis model by enhancing the immune function of macrophages and T cells in the blood, thereby reinforcing the body's ability to fight cancer with no additional harm to the mice (Figs. 5 and 6). The effects of the four component drugs, MSC (Avery and Hoffmann, 2018; Li et al., 2020; Ganash, 2021; Jiang et al., 2021), VES (Kontek et al., 2014; Huang et al., 2021), β-Ca (Satomi and Nishino, 2013; Kim et al., 2014), and Lys (Roomi et al., 2005; Ibrahim-Hashim et al., 2011; Kirchhain et al., 2021), are known, and the drugs are widely used. HPLC data showed that their combination would not produce new chemicals (Fig. S2). Therefore, MVBL retains the original biological activity and high safety. The combination and rational application of existing drugs and nutrition for more effective treatment of tumors are currently ignored (Hébert et al., 2014; Barrett et al., 2020).

5 Conclusions

Our findings showed that MVBL may significantly improve the physiological and nutritional status and organ function of patients after surgery, chemotherapy, and radiotherapy. Moreover, MVBL can inhibit tumor metastasis and improve immune function, and be used as an adjuvant drug to improve treatment effects.

Acknowledgments

This work was supported by the National Natural Science Foundation of China (Nos. 81961138017 and 81703555),

the Natural Science Foundation of Fujian Province (Nos. 2021J011046 and 2020J01859), the Young and Middle-aged Teacher Education Research Project of Fujian Province (No. JAT200412), the Science and Technology Planning Projects of Fuzhou (No. 2021S094), the Science and Technology Planning Projects of Fuzhou Institute of Oceanography (No. 2021F08), the Belt & Road Program (No. KXPT-2021-3, CAST), and the Ministry of Science and Technology of China (No. 2015CB931804).

Author contributions

Yunlong CHENG, Yusheng LU, and Lee JIA planned the study. Yunlong CHENG, Shu LIAN, Shuhui LI, Yusheng LU, Jie WANG, Xiaoxiao DENG, and Shengyi ZHAI performed cell experiments and collected data. Shu LIAN, Shuhui LI, and Yusheng LU analyzed and interpreted data. Yunlong CHENG, Shu LIAN, and Lee JIA drafted manuscript. All the authors have read and approved the final manuscript, and therefore, have full access to all the data in the study and take responsibility for the integrity and security of the data.

Compliance with ethics guidelines

Yunlong CHENG, Shu LIAN, Shuhui LI, Yusheng LU, Jie WANG, Xiaoxiao DENG, Shengyi ZHAI, and Lee JIA declare that they have no conflict of interest.

All institutional and national guidelines for the care and use of laboratory animals were followed. All animal care and experimental procedures were approved by the Minjiang University Institutional Animal Care and Use Committee (No. 20221114R).

References

Abu Samaan TM, Samec M, Liskova A, et al., 2019. Paclitaxel's mechanistic and clinical effects on breast cancer. *Biomolecules*, 9(12):789. https://doi.org/10.3390/biom9120789

Avery JC, Hoffmann PR, 2018. Selenium, selenoproteins, and immunity. *Nutrients*, 10(9):1203. https://doi.org/10.3390/nu10091203

Barrett M, Uí Dhuibhir P, Njoroge C, et al., 2020. Diet and nutrition information on nine national cancer organisation websites: a critical review. *Eur J Cancer Care (Engl)*, 29(5):e13280. https://doi.org/10.1111/ecc.13280

Cheung EC, Denicola GM, Nixon C, et al., 2020. Dynamic ROS control by TIGAR regulates the initiation and progression of pancreatic cancer. *Cancer Cell*, 37(2):168-182.e4. https://doi.org/10.1016/j.ccell.2019.12.012

Crowder SW, Horton LW, Lee SH, et al., 2013. Passage-dependent cancerous transformation of human mesenchymal stem cells under carcinogenic hypoxia. *FASEB J*, 27(7): 2788-2798. https://doi.org/10.1096/fj.13-228288

Dikic I, Elazar Z, 2018. Mechanism and medical implications of mammalian autophagy. *Nat Rev Mol Cell Biol*, 19(6): 349-364. https://doi.org/10.1038/s41580-018-0003-4

Fang YZ, Yang S, Wu GY, 2002. Free radicals, antioxidants, and nutrition. *Nutrition*, 18(10):872-879. https://doi.org/10.1016/S0899-9007(02)00916-4

Ganash MA, 2021. Anticancer potential of ascorbic acid and inorganic selenium on human breast cancer cell line MCF-7 and colon carcinoma HCT-116. *J Cancer Res Ther*, 17(1): 122-129. https://doi.org/10.4103/jcrt.JCRT_989_17

Guo YY, Xiao YY, Guo HC, et al., 2021. The anti-dysenteric drug fraxetin enhances anti-tumor efficacy of gemcitabine and suppresses pancreatic cancer development by antagonizing STAT3 activation. *Aging (Albany NY)*, 13(14): 18545-18563. https://doi.org/10.18632/aging.203301

Hébert JR, Hurley TG, Steck SE, et al., 2014. Considering the value of dietary assessment data in informing nutrition-related health policy. *Adv Nutr*, 5(4):447-455. https://doi.org/10.3945/an.114.006189

Huang XL, Neckenig M, Sun JT, et al., 2021. Vitamin E succinate exerts anti-tumour effects on human cervical cancer cells via the CD47-SIRPα pathway both *in vivo* and *in vitro*. *J Cancer*, 12(13):3877-3886. https://doi.org/10.7150/jca.52315

Ibrahim-Hashim A, Wojtkowiak JW, de Lourdes Coelho Ribeiro M, et al., 2011. Free base lysine increases survival and reduces metastasis in prostate cancer model. *J Cancer Sci Ther*, Suppl 1(4):JCST-S1-004.

Jiang Q, 2017. Natural forms of vitamin E as effective agents for cancer prevention and therapy. *Adv Nutr*, 8(6):850-867. https://doi.org/10.3945/an.117.016329

Jiang ZW, Chi JH, Li H, et al., 2021. Effect of chitosan oligosaccharide-conjugated selenium on improving immune function and blocking gastric cancer growth. *Eur J Pharmacol*, 891:173673. https://doi.org/10.1016/j.ejphar.2020.173673

Kim YS, Lee HA, Lim JY, et al., 2014. β-Carotene inhibits neuroblastoma cell invasion and metastasis *in vitro* and *in vivo* by decreasing level of hypoxia-inducible factor-1α. *J Nutr Biochem*, 25(6):655-664. https://doi.org/10.1016/j.jnutbio.2014.02.006

Kirchhain A, Zubrienė A, Kairys V, et al., 2021. Biphenyl substituted lysine derivatives as recognition elements for the matrix metalloproteinases MMP-2 and MMP-9. *Bioorg Chem*, 115:105155. https://doi.org/10.1016/j.bioorg.2021.105155

Kontek R, Jakubczak M, Matlawska-Wasowska K, 2014. The antioxidants, vitamin A and E but not vitamin C and melatonin enhance the proapoptotic effects of irinotecan in cancer cells *in vitro*. *Toxicol in Vitro*, 28(2):282-291. https://doi.org/10.1016/j.tiv.2013.11.007

Li CH, Li YF, Yao TT, et al., 2020. Wireless electrochemotherapy by selenium-doped piezoelectric biomaterials to enhance cancer cell apoptosis. *ACS Appl Mater Interfaces*, 12(31):34505-34513.

https://doi.org/10.1021/acsami.0c04666

Liu XY, Pei CY, Yan S, et al., 2015. NADPH oxidase 1-dependent ROS is crucial for TLR4 signaling to promote tumor metastasis of non-small cell lung cancer. *Tumor Biol*, 36(3):1493-1502. https://doi.org/10.1007/s13277-014-2639-9

Ma L, Liu L, Ma YC, et al., 2017. The role of E-cadherin/β-catenin in hydroxysafflor yellow a inhibiting adhesion, invasion, migration and lung metastasis of hepatoma cells. *Biol Pharm Bull*, 40(10):1706-1715. https://doi.org/10.1248/bpb.b17-00281

Marian M, August DA, 2014. Prevalence of malnutrition and current use of nutrition support in cancer patient study. *J Parenter Enteral Nutr*, 38(2):163-165. https://doi.org/10.1177/0148607113506940

Martínez-Reyes I, Chandel NS, 2021. Cancer metabolism: looking forward. *Nat Rev Cancer*, 21(10):669-680. https://doi.org/10.1038/s41568-021-00378-6

Ørskov H, Flyvbjerg A, 2000. Selenium and human health. *Lancet*, 356(9233):942-943. https://doi.org/10.1016/S0140-6736(05)73926-X

Prasad S, Gupta SC, Tyagi AK, 2017. Reactive oxygen species (ROS) and cancer: role of antioxidative nutraceuticals. *Cancer Lett*, 387:95-105. https://doi.org/10.1016/j.canlet.2016.03.042

Roomi MW, Ivanov V, Kalinovsky T, et al., 2005. In vitro and in vivo antitumorigenic activity of a mixture of lysine, proline, ascorbic acid, and green tea extract on human breast cancer lines MDA-MB-231 and MCF-7. *Med Oncol*, 22(2):129-138. https://doi.org/10.1385/MO:22:2:129

Satomi Y, Nishino H, 2013. Inhibition of the enzyme activity of cytochrome P450 1A1, 1A2 and 3A4 by fucoxanthin, a marine carotenoid. *Oncol Lett*, 6(3):860-864. https://doi.org/10.3892/ol.2013.1457

Shimojo Y, Akimoto M, Hisanaga T, et al., 2013. Attenuation of reactive oxygen species by antioxidants suppresses hypoxia-induced epithelial-mesenchymal transition and metastasis of pancreatic cancer cells. *Clin Exp Metastasis*, 30(2):143-154. https://doi.org/10.1007/s10585-012-9519-8

Siegel RL, Miller KD, Fuchs HE, et al., 2022. Cancer statistics, 2022. *CA Cancer J Clin*, 72(1):7-33. https://doi.org/10.3322/caac.21708

Su X, Shen Z, Yang Q, et al., 2019. Vitamin C kills thyroid cancer cells through ROS-dependent inhibition of MAPK/ERK and PI3K/AKT pathways via distinct mechanisms. *Theranostics*, 9(15):4461-4473. https://doi.org/10.7150/thno.35219

Wang YW, Qi H, Liu Y, et al., 2021. The double-edged roles of ROS in cancer prevention and therapy. *Theranostics*, 11(10):4839-4857. https://doi.org/10.7150/thno.56747

Zhang T, Zhu XY, Wu HC, et al., 2019. Targeting the ROS/PI3K/AKT/HIF-1α/HK2 axis of breast cancer cells: combined administration of Polydatin and 2-Deoxy-d-glucose. *J Cell Mol Med*, 23(5):3711-3723. https://doi.org/10.1111/jcmm.14276

Zhou MG, Wang HD, Zeng XY, et al., 2019. Mortality, morbidity, and risk factors in China and its provinces, 1990–2017: a systematic analysis for the Global Burden of Disease Study 2017. *Lancet*, 394(10204):1145-1158. https://doi.org/10.1016/S0140-6736(19)30427-1

Zhou X, Ji WJ, Zhu Y, et al., 2007. Enhancement of endogenous defenses against ROS by supra-nutritional level of selenium is more safe and effective than antioxidant supplementation in reducing hypertensive target organ damage. *Med Hypotheses*, 68(5):952-956. https://doi.org/10.1016/j.mehy.2006.09.058

Supplementary information

Figs. S1–S7